

Giant Nernst Effect due to Fluctuating Cooper Pairs in Superconductors

M. N. Serbyn,¹ M. A. Skvortsov,^{1,*} A. A. Varlamov,² and Victor Galitski³

¹*Landau Institute for Theoretical Physics, Chernogolovka, Moscow Region, 142432, Russia*

²*COHERENTIA-INFN, CNR, Viale del Politecnico 1, I-00133 Rome, Italy*

³*Joint Quantum Institute and CNAM, Department of Physics, University of Maryland, College Park, Maryland 20742-4111, USA*

(Received 27 June 2008; revised manuscript received 10 January 2009; published 9 February 2009)

A theory of the fluctuation-induced Nernst effect is developed for a two-dimensional superconductor in a perpendicular magnetic field. First, we derive a simple phenomenological formula for the Nernst coefficient, which naturally explains the giant Nernst signal due to fluctuating Cooper pairs. The latter signal is shown to be large even far from the transition and may exceed by orders of magnitude the Fermi liquid terms. We also present a complete microscopic calculation of the Nernst coefficient for arbitrary magnetic fields and temperatures, which is based on the Matsubara-Kubo formalism. It is shown that the magnitude and the behavior of the Nernst signal observed experimentally in disordered superconducting films can be well understood on the basis of superconducting fluctuation theory.

DOI: 10.1103/PhysRevLett.102.067001

PACS numbers: 74.40.+k, 72.15.Jf, 74.25.Fy

A series of recent experimental studies have revealed anomalously strong thermomagnetic signal in the normal state of the high-temperature superconductors [1–8] and disordered superconducting (SC) films [9,10]. In the pioneering experiment [1], Xu *et al.* observed a sizeable Nernst effect in the $\text{La}_{2-x}\text{Sr}_x\text{CuO}_4$ compounds up to 130 K, well above the transition temperature, T_c . This and further similar experiments on the cuprates have sparked theoretical interest in the thermomagnetic phenomena. Theoretical approaches to the anomalously large Nernst-Ettingshausen effect currently include models based on the proximity to a quantum critical point [11], vortex motion in the pseudogap phase [2,12,13], as well as a SC fluctuation scenario [14–16]. While the two former theories are specific to the cuprate superconductors, the latter scenario should apply to other more conventional SC systems as well. Very recently, a large Nernst coefficient was observed in the normal state of disordered superconducting films [9,10]. These films are likely to be well-described by the usual BCS model and, hence, the new experimental measurements provide an indication that the SC fluctuations are likely to be the key to understanding the underlying physics of the giant thermomagnetic response.

Various groups have previously calculated the fluctuation-induced Nernst coefficient in the vicinity of the classical transition [14–18]. However, these analyses were limited to the case of very weak magnetic fields and temperatures close to T_c . In experiment, however, other parts of the phase diagram (in particular strong fields) are obviously important and how the quantized motion of fluctuating Cooper pairs would figure into the thermomagnetic response has remained unclear. In this Letter we clarify this physics, explaining the origin of the giant fluctuation Nernst-Ettingshausen effect, and develop a complete microscopic theory of Gaussian SC fluctuations at arbitrary magnetic fields and temperatures.

We start with a qualitative discussion of the Nernst-Ettingshausen effect. Consider a conductor in the presence of a magnetic field, H_z , and electric field, E_y , directed along the z and y axes, respectively. The charged carriers subject to these crossed fields acquire a drift velocity $\bar{v}_x = cE_y/H_z$ in the x direction. That would result in the appearance of a transverse current $j_x = ne\bar{v}_x$. When the circuit is broken, no current flows, and the drift of carriers is prevented by the spacial variation of the electric potential: $\nabla_x\varphi = -E_x = (nec/\sigma)(E_y/H_z)$, where σ is the conductivity. Because of electroneutrality, this generates the gradient of the chemical potential: $\nabla_x\mu(n, T) + e\nabla_x\varphi = 0$, which corresponds to the appearance of the temperature gradient $\nabla_x T = (d\mu/dT)^{-1}\nabla_x\mu$ along the x direction. Hence, the Nernst coefficient can be expressed in terms of the full temperature derivative of the chemical potential:

$$\nu_N \equiv \frac{E_y}{(-\nabla_x T)H_z} = \frac{\sigma}{ne^2c} \frac{d\mu}{dT}. \quad (1)$$

E.g., in a degenerate electron gas, the chemical potential $\mu(T) = \mu_0 - (\pi^2 T^2/6)(d\ln\nu/d\mu)$, where $\nu(\mu)$ is the density of states, and one easily reproduces the value of the Nernst coefficient in a normal metal [19,20]: $\nu_N = (\pi^2 T/3mc)(d\tau/d\mu)$, where τ is the elastic scattering time (here and below $\hbar = k_B = 1$). Thus the Nernst effect in metals is small due to the large value of the Fermi energy.

The simple form of Eq. (1) suggests that in order to get a large Nernst signal, a strong temperature dependence of the chemical potential of carriers is required. That can be achieved in the vicinity of the SC transition where fluctuating Cooper pairs appear besides normal electrons. In two dimensions (2D), the concentration of these excitations is $n_{\text{c.p.}}^{(2)}(T) = (mT_c/\pi) \ln[T_c/(T - T_c)]$ [21], which corresponds to the chemical potential $\mu_{\text{c.p.}}(T) = T_c - T$. Since $d\mu_{\text{c.p.}}/dT = -1$, the fluctuation contribution to the Nernst signal exceeds parametrically the Fermi liquid

term. In this sense it is similar to the fluctuation diamagnetism (which also exceeds the Landau/Pauli terms and is effectively a correction to the perfect diamagnetism of a superconductor). Substituting the known expression for paraconductivity in a magnetic field, $\sigma_{\parallel} = (e^2/2\epsilon)F(\epsilon/2\tilde{h})$ [21], into Eq. (1), one finds the value of the Nernst coefficient in the Ginzburg-Landau (GL) region:

$$\nu_N^{(\text{GL})} \sim \frac{1}{mc} \frac{F(x)}{T - T_c} \sim \begin{cases} [mc(T - T_c)]^{-1}, & x \gg 1, \\ (meDH)^{-1}, & x \ll 1, \end{cases} \quad (2)$$

$$F(x) = x^2[\psi(1/2 + x) - \psi(x) - 1/(2x)], \quad (3)$$

where $x = \epsilon/2\tilde{h}$, $\epsilon = \ln(T/T_c)$ and $\tilde{h} = H/\tilde{H}_{c2}(0)$ are the reduced temperature and magnetic field, $\tilde{H}_{c2}(0) = 4cT_c/\pi eD$ is the linearly extrapolated value of the upper critical field, and D is the diffusion coefficient. The estimate (2) corresponds to the results [14,17].

We now proceed with the microscopic calculation of the Nernst coefficient, $\nu_N(T, H) = R_{\square}\beta^{xy}/H$, and first recall a deep relation between the fluctuation Nernst effect and magnetization as emphasized in Refs. [14,22,23]: In the presence of a magnetic field, the measurable transport heat current \mathbf{j}_{tr}^Q differs from the microscopic heat current \mathbf{j}^Q by the circular magnetization current $\mathbf{j}_M^Q = c\mathbf{M} \times \mathbf{E}$, where \mathbf{M} is the induced magnetization. As a result, the thermoelectric tensor $\beta^{\alpha\beta}$ relating $j_{\text{tr}}^{Q\alpha} = T\beta^{\alpha\beta}E^\beta$ with the applied electric field \mathbf{E} can be found as a sum of the kinetic, $\tilde{\beta}^{\alpha\beta}$, and thermodynamic, $\beta_M^{\alpha\beta}$, contributions:

$$\beta^{\alpha\beta} = \tilde{\beta}^{\alpha\beta} + \beta_M^{\alpha\beta}, \quad \beta_M^{\alpha\beta} = \epsilon^{\alpha\beta\gamma} cM^\gamma/T. \quad (4)$$

The term $\tilde{\beta}^{\alpha\beta}$ can be expressed via the Matsubara correlator of the electric and heat currents, $Q^{\alpha\beta}(\omega_\nu) = \langle j^{e\alpha}(-\omega_\nu)j^{Q\beta}(\omega_\nu) \rangle$, by analytic continuation to real frequencies: $\tilde{\beta}^{\alpha\beta} = T^{-1}\lim_{\omega \rightarrow 0} \text{Im}Q^{\alpha\beta}(-i\omega + 0)/\omega$, while the term $\beta_M^{\alpha\beta}$ accounts for the magnetization heat current \mathbf{j}_M^Q . The fluctuation magnetization, $M(T, H)$, has been calculated previously in the GL region [21,24,25] and at low temperatures [26].

Our goal now is to evaluate the linear response operator $Q^{xy}(\omega_\nu)$. We perform calculations in the Landau basis, which guarantees that gauge invariance is preserved and allows us to access the high-field regime [26]. The fluctuation part of the correlator $Q^{xy}(\omega_\nu)$ is generally represented by ten diagrams [21,26]. However, in the case of the Nernst effect, the Maki-Thompson contribution can be shown to be exactly zero and some of the DOS diagrams

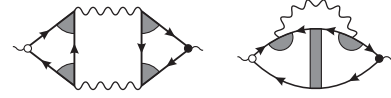


FIG. 1. The Aslamazov-Larkin (AL) and density-of-states (DOS) diagrams for the thermoelectric response $\tilde{\beta}^{xy}$. The DOS diagram has a symmetric counterpart. The white and black circles correspond to the different heat and electric vertices, the shadowed blocks represent Cooperons, and the wavy lines denote the fluctuation propagator (see text). All objects on these graphs are generally matrices in the Landau basis.

turn out to be less singular: The graphs containing three Cooperons (see Fig. 1) are dominant. The positive Aslamazov-Larkin (AL) term dominates in the classical GL region and competes with the negative density-of-states (DOS) contribution everywhere else. These AL and DOS contributions, and the fluctuation magnetization are given by

$$Q_{\text{AL}}^{xy}(\omega_\nu) = -4\nu_H T \sum_{\Omega_k} \sum_{n,m} \hat{q}_{mn}^x B_{nm}^{(e)} L_n(\Omega_k) \times \hat{q}_{nm}^y B_{nm}^{(Q)} L_m(\Omega_{k+\nu}), \quad (5)$$

$$2Q_{\text{DOS}}^{xy}(\omega_\nu) = 4\nu_H T \sum_{\Omega_k} \sum_{n,m} \hat{q}_{mn}^x \Sigma_{nm}^{(e,Q)} \hat{q}_{nm}^y L_n(\Omega_k), \quad (6)$$

$$M^z = -\frac{\partial}{\partial H} \nu_H T \sum_{\Omega_k} \sum_n \ln L_n^{-1}(\Omega_k). \quad (7)$$

Here $L_n(\Omega_k) = -\nu^{-1}[\ln(T/T_c) + \psi_n(|\Omega_k|) - \psi(1/2)]^{-1}$ is the fluctuation propagator, $\psi_n(\Omega)$ is a shorthand notation for $\psi[1/2 + (\Omega + \alpha_n)/4\pi T]$, with $\alpha_n = (4eDH/c) \times (n + 1/2)$ being the Landau spectrum, $\nu_H = eH/\pi c$, and the matrix elements of the momentum operator in the Landau basis are given by $\hat{q}_{mn}^\alpha = \sqrt{eH/c}(u_\alpha \sqrt{m} \delta_{m,n+1} + u_\alpha^* \sqrt{n} \delta_{n,m+1})$, where $u_x = i, u_y = 1$.

The blocks B and Σ entering Eqs. (5) and (6) are made of Green functions, Cooperons, and electric and heat vertices. We note here that there exists a long-standing controversy of the proper definition of the heat current and, more generally, the applicability of Kubo-type linear response theory for thermal transport. In our microscopic calculations, we do assume that the latter holds and use the standard definition of the heat current [21], with the heat vertex $i(\epsilon_e + \epsilon_{e+\nu})\mathbf{v}/2$. Then we find ($\omega_\nu \geq 0$):

$$B_{nm}^{(e)}(\Omega_k, \omega_\nu) = e\nu D \left[\frac{\psi_m(\omega_\nu + |\Omega_k|) - \psi_n(|\Omega_k|)}{\omega_\nu + \alpha_m - \alpha_n} + \frac{\psi_n(\omega_\nu + |\Omega_{k+\nu}|) - \psi_m(|\Omega_{k+\nu}|)}{\omega_\nu - \alpha_m + \alpha_n} \right], \quad (8)$$

$$B_{nm}^{(Q)}(\Omega_k, \omega_\nu) = -\frac{i\nu D}{2} \left[\frac{(\Omega_k - \alpha_m)\psi_n(|\Omega_k| + \omega_\nu) - (\Omega_{k+\nu} - \alpha_n)\psi_n(|\Omega_k|)}{\omega_\nu + \alpha_m - \alpha_n} + \frac{(\Omega_{k+\nu} + \alpha_n)\psi_n(|\Omega_{k+\nu}| + \omega_\nu) - (\Omega_k + \alpha_m)\psi_m(|\Omega_{k+\nu}|)}{\omega_\nu + \alpha_n - \alpha_m} \right], \quad (9)$$

$$\Sigma_{nm}^{(e,Q)}(\Omega_k, \omega_\nu) = -ievD^2 \left[\frac{\Omega_{k+\nu} - \alpha_n}{\omega_\nu + \alpha_m - \alpha_n} \psi'_n(|\Omega_k|) - \frac{\Omega_{k+\nu} + \alpha_n}{\omega_\nu - \alpha_m + \alpha_n} \psi'_n(|\Omega_{k+\nu}| + \omega_\nu) - \frac{\Omega_k - \alpha_m}{(\omega_\nu + \alpha_m - \alpha_n)^2} \right. \\ \left. \times (\psi_m(|\Omega_k| + \omega_\nu) - \psi_n(|\Omega_k|)) + \frac{\Omega_k + \alpha_m}{(\omega_\nu - \alpha_m + \alpha_n)^2} (\psi_n(|\Omega_{k+\nu}| + \omega_\nu) - \psi_m(|\Omega_{k+\nu}|)) \right]. \quad (10)$$

The general calculation of Eqs. (5)–(7) and their analytic continuation to real frequencies is straightforward but cumbersome. However, one can identify nine qualitatively different regions of the phase diagram (Fig. 2), where the asymptotic behavior has a simple analytical form. Before proceeding to the corresponding details, we emphasize that the result for the Nernst coefficient is universal in the sense that the function $\beta^{xy}(T, H)$ depends only on T/T_c and $H/H_{c2}(0)$, but not the elastic scattering time τ (unlike conductivity). This universality is due to the magnetization contribution, β_M^{xy} , which regularizes the otherwise divergent (and thus τ -dependent) terms in $\tilde{\beta}^{xy}$. These remarkable cancellations between the two physically distinct terms taking place in a wide parameter range provide a strong evidence that the standard definition of the heat vertices is indeed appropriate to describe the effect.

We start by discussing the classical regime close to the critical temperature T_c : The regions I, II, III in Fig. 2 are characterized by $\epsilon = \ln(T/T_c) \ll 1$ and $\tilde{h} = H/\tilde{H}_{c2}(0) \ll 1$. In these domains, only the classical AL contribution is important and is given by [cf. Eq. (2)]: $\tilde{\beta}^{xy} = 2\beta_0 F(x)/x$, where $x = \epsilon/2\tilde{h}$, $\beta_0 = k_B e / \pi \hbar = 6.68$ nA/K is the quantum of thermoelectric conductance, and the function $F(x)$ is given by Eq. (3). The magnetization contribution is

$$\beta_M^{xy} = \beta_0 \left[\ln \frac{\Gamma(1/2 + x)}{\sqrt{2\pi}} - x \psi(1/2 + x) + x \right]. \quad (11)$$

In the limit of vanishingly small magnetic fields $\tilde{h} \ll \epsilon$ (region I), we find $\tilde{\beta}^{xy} = \beta_0(\tilde{h}/2\epsilon)$, which is 2 times larger than the result of Refs. [14,15,21]. The additional factor is due to the complicated analytic structure of the heat-current block (9) overlooked in the previous diagrammatic calculations of Refs. [14,15,21], but properly accounted for in Ref. [18]. Note that our result for $\tilde{\beta}^{xy}$ also differs by a factor of 2 from the prediction of the phenomenological time-dependent GL approach [21]. This difference may be related to a more fundamental issue (as compared to a calculational mistake) and may signal, e.g., a problem with the definition of the heat currents within time-dependent GL theory or/and diagrammatics. The exact origin of the factor-of-two remains unclear at this stage. In the region I we obtain

$$\beta_I^{xy} = \beta_0 \frac{\tilde{h}}{3\epsilon} = \beta_0 \frac{\pi e D H}{12c(T - T_c)}, \quad \tilde{h} \ll \epsilon \ll 1, \quad (12)$$

which is 4 times larger than the result of Refs. [14,15,21]. In the limit $\epsilon \ll \tilde{h}$ (region II), and close to the transition line, at $\tilde{h} + \epsilon \ll \tilde{h}$ (region III), we find

$$\beta_{II}^{xy} = \beta_0 [1 - (\ln 2)/2], \quad \epsilon \ll \tilde{h} \ll 1; \quad (13)$$

$$\beta_{III}^{xy} = \beta_0 \frac{\tilde{h}}{\epsilon + \tilde{h}} = \beta_0 \frac{H_{c2}(T)}{H - H_{c2}(T)}, \quad \epsilon + \tilde{h} \ll \tilde{h} \ll 1. \quad (14)$$

Now we turn to the low-temperature regime close to the upper critical field $H_{c2}(0) = \pi c T_c / 2 \gamma e D$ (regions IV, V, VI in Fig. 2), where $\gamma = 1.78 \dots$. Here the role of the magnetization term becomes crucial: The cancellation of the $1/T$ divergence of $\tilde{\beta}^{xy}$ by $\beta_M^{xy} = c M^z / T$ ensures that the third law of thermodynamics holds, making β^{xy} finite as $T \rightarrow 0$. In the purely quantum limit of vanishing temperature ($t \ll \eta$, region IV), β^{xy} is negative:

$$\beta_{IV}^{xy} = -\frac{2\beta_0 \gamma t}{9\eta} = -\frac{\beta_0 \pi c T / 9 e D}{H - H_{c2}(0)}, \quad t \ll \eta \ll 1. \quad (15)$$

This change of sign is due to the DOS contribution being numerically larger than the positive AL term [26]. In the quantum-to-classical crossover region, where H tends to $H_{c2}(t)$ but remains limited as $t^2 / \ln(1/t) \ll \eta \ll t$ (region V), the coefficient β^{xy} is positive:

$$\beta_V^{xy} = \beta_0 \ln(t/\eta), \quad t^2 / \ln(1/t) \ll \eta \ll t \ll 1. \quad (16)$$

Near $H_{c2}(t)$ ($\eta \ll t^2 / \ln(1/t)$, region VI), we find:

$$\beta_{VI}^{xy} = 8\beta_0 \gamma^2 t^2 / 3\eta, \quad \eta \ll t^2 / \ln(1/t) \ll 1. \quad (17)$$

We also address the full classical region just above the transition line, which covers a wide range of temperatures and magnetic fields ($\eta \ll 1$, region VII). Here

$$\beta_{VII}^{xy} = \frac{\beta_0}{\eta} \left[1 + \frac{h}{4\gamma t} \frac{\psi''(1/2 + h/4\gamma t)}{\psi'(1/2 + h/4\gamma t)} \right], \quad \eta \rightarrow 0, \quad (18)$$

with $h = H/H_{c2}(0)$. Close to T_c , Eq. (18) matches Eq. (14), while in the limit $T \rightarrow 0$ it matches Eq. (17) provided that $\eta \ll t^2 / \ln(1/t)$.

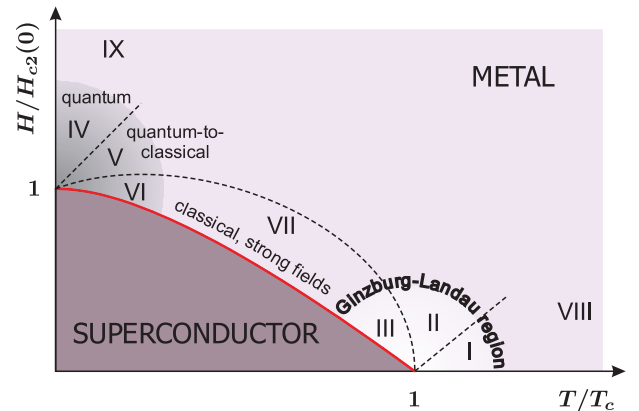


FIG. 2 (color online). Different asymptotic regions for the fluctuation Nernst effect on the H - T phase diagram.

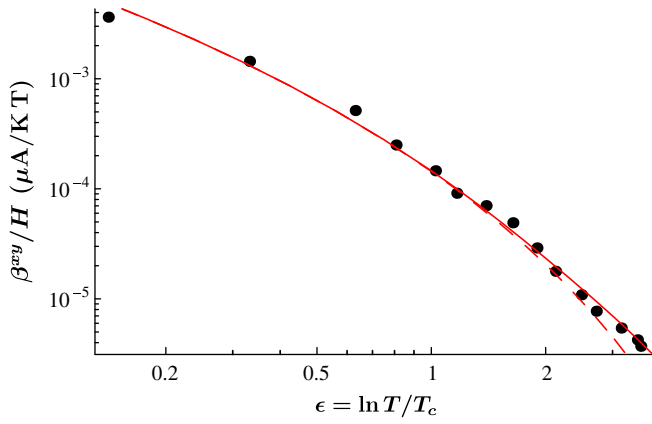


FIG. 3 (color online). Comparison with experiment. Circles: experimental data for $\lim_{H \rightarrow 0} \beta^{xy}/H$ vs $\epsilon = \ln T/T_c$ obtained for the 12.5-nm-thick $\text{Nb}_{0.15}\text{Si}_{0.85}$ film [9]. Dashed line: theoretical prediction for the strictly 2D geometry. Solid line: theoretical prediction for the real sample [9].

Finally, we address the regions VIII and IX far from the transition line. In this limit, the Kubo contribution $\tilde{\beta}^{xy}$ diverges as $[\ln \ln(1/T_c \tau) - \ln \ln \max(h, t)]$, with $1/\tau$ playing the role of the ultraviolet cutoff of the Cooperon modes. Remarkably, the same divergence of the opposite sign occurs in the magnetization contribution β_M^{xy} . Hence, β^{xy} remains τ independent:

$$\beta_{\text{VIII}}^{xy} = \beta_0 \frac{eDH}{6\pi cT \ln(T/T_c)}, \quad (1, h) \ll t; \quad (19)$$

$$\beta_{\text{IX}}^{xy} = \beta_0 \frac{\pi cT}{12eDH \ln[H/H_c2(0)]}, \quad (1, t) \ll h. \quad (20)$$

We see that even far from the transition the fluctuation Nernst signal can be comparable or parametrically larger than the Fermi liquid terms. In fact, it is conceivable that in some materials the Cooper channel contribution to thermal transport dominates even in the absence of any superconducting transition (e.g., if it is “hidden” by another order).

Plotted in Fig. 3 is a comparison between our theory and the experimentally measured Nernst coefficient [9] for a $\text{Nb}_{0.15}\text{Si}_{0.85}$ film of thickness $d = 12.5$ nm. The dashed line corresponds to the coefficient $\lim_{H \rightarrow 0} \beta^{xy}/H$ in a wide range of temperatures up to $30T_c$. We used the diffusion coefficient $D = 0.087$ cm^2/s which is 60% of that reported in Ref. [9] (with $k_F l \sim 1$, the precise determination of D is questionable). Note that far from the transition point ($\epsilon > 2$), the SC coherence length $\xi(T)$ becomes shorter than d and 3D nature of diffusion manifests itself. It can be described by substituting $\alpha_n \rightarrow \alpha_n + D(\pi p/d)^2$ and performing an additional summation over $p = 0, 1, \dots$ in Eqs. (5)–(7). The resulting curve is shown in Fig. 3 by the solid line.

In summary, we have developed a complete microscopic theory of the fluctuation Nernst effect in a 2D superconductor. Our results provide a natural explanation for a large

Nernst signal observed in SC films [9,10] and probably should be relevant to the cuprates. Another interesting theoretical prediction is a slow decay of the transverse thermoelectric response away from the transition line, which is expected to persist well into the metallic phase.

We are grateful to H. Aubin, M. Feigel'man, and A. Kavokin for useful discussions. M.N.S. acknowledges support from Dynasty Foundation and hospitality of the University Paris-Sud. V.G. acknowledges BU visitors program's hospitality. The work of M.N.S. and M.A.S. was partially supported by RFBR Grant No. 07-02-00310.

Note added in proof.—In a very recent preprint [27], the fluctuation Nernst effect has been analyzed within the Keldysh formalism. Results of Ref. [27] qualitatively coincide with our results, differing in some numerical factors of order 1 in several asymptotic regions.

*skvor@itp.ac.ru

- [1] Z. A. Xu *et al.*, Nature (London) **406**, 486 (2000).
- [2] Y. Wang *et al.*, Phys. Rev. B **64**, 224519 (2001).
- [3] Y. Wang *et al.*, Phys. Rev. Lett. **88**, 257003 (2002).
- [4] C. Capan *et al.*, Phys. Rev. Lett. **88**, 056601 (2002).
- [5] H. H. Wen *et al.*, Europhys. Lett. **63**, 583 (2003).
- [6] Z. A. Xu *et al.*, Phys. Rev. B **72**, 144527 (2005).
- [7] Y. Wang, L. Li, and N. P. Ong, Phys. Rev. B **73**, 024510 (2006).
- [8] P. Li and R. L. Greene, Phys. Rev. B **76**, 174512 (2007).
- [9] A. Pourret *et al.*, Nature Phys. **2**, 683 (2006).
- [10] A. Pourret *et al.*, Phys. Rev. B **76**, 214504 (2007).
- [11] S. A. Hartnoll *et al.*, Phys. Rev. B **76**, 144502 (2007).
- [12] D. Podolsky, S. Raghu, and A. Vishwanath, Phys. Rev. Lett. **99**, 117004 (2007).
- [13] S. Raghu *et al.*, Phys. Rev. B **78**, 184520 (2008).
- [14] I. Ussishkin, S. L. Sondhi, and D. A. Huse, Phys. Rev. Lett. **89**, 287001 (2002).
- [15] I. Ussishkin, Phys. Rev. B **68**, 024517 (2003).
- [16] I. Ussishkin and S. L. Sondhi, Int. J. Mod. Phys. B **18**, 3315 (2004).
- [17] S. Ullah and A. T. Dorsey, Phys. Rev. Lett. **65**, 2066 (1990); Phys. Rev. B **44**, 262 (1991).
- [18] M. Yu. Reizer and A. V. Sergeev, Phys. Rev. B **50**, 9344 (1994).
- [19] E. H. Sondheimer, Proc. R. Soc. A **193**, 484 (1948).
- [20] We assume white-noise disorder, i.e., $\tau(\epsilon)\nu(\epsilon) = \text{const}$.
- [21] A. I. Larkin and A. A. Varlamov, in *Theory of Fluctuations in Superconductors*, (Oxford University Press, New York, 2002).
- [22] L. Li *et al.*, Europhys. Lett. **72**, 451 (2005).
- [23] N. R. Cooper, B. I. Halperin, and I. M. Ruzin, Phys. Rev. B **55**, 2344 (1997).
- [24] J. Kurkijärvi, V. Ambegaokar, and G. Eilenberger, Phys. Rev. B **5**, 868 (1972).
- [25] R. A. Klemm, M. R. Beasley, and A. Luther, Phys. Rev. B **8**, 5072 (1973).
- [26] V. M. Galitski and A. I. Larkin, Phys. Rev. B **63**, 174506 (2001).
- [27] K. Michaeli and A. M. Finkel'stein, arXiv:0812.4268.